JOURNAL OF CATALYSIS **131**, 167–177 (1991)

FT–IR Study of the Surface Properties of the Spinels $NiAl_2O_4$ and $CoAl_2O_4$ in Relation to Those of Transitional Aluminas

GUIDO BUSCA, VINCENZO LORENZELLI, VICENTE SANCHEZ ESCRIBANO,[1] AND RICCARDO GUIDETTI

Istituto di Chimica, Facoltà di Ingegneria, Università di Genova, Piazzale Kennedy, 16129 Genova, Italy

Received September 28, 1990; revised March 25, 1991

The surface chemistry of δ-Al_2O_3, $NiAl_2O_4$, and $CoAl_2O_4$ has been investigated comparatively by FT–IR spectroscopy using adsorbed carbon monoxide and pyridine as probe molecules. The surface OHs of the inverse spinel $NiAl_2O_4$ are very similar to those of δ-Al_2O_3 and other transitional aluminas while those of $CoAl_2O_4$ are different and resemble those of other normal spinels. Both carbon monoxide and pyridine adsorption provide evidence for the presence of tetrahedral Al^{3+} ions exposed on the surface of the inverse spinel $NiAl_2O_4$. On the normal spinel $CoAl_2O_4$ octahedral Al^{3+} ions predominate with respect to the tetrahedral ones, also present because of partial inversion. Ni^{2+} and Co^{2+} ions are also detected on the respective surfaces. Slight modifications to the literature criteria are suggested for the assignments of the IR bands to surface OHs and of adsorbed pyridine on aluminas.

INTRODUCTION

Alumina is a polymorphic material that finds numerous applications in heterogeneous catalysis and adsorption (*1–3*). The most stable form thermodynamically is the hexagonal phase corundum (α-Al_2O_3) whose applications in catalysis are related to its surface inertness and its mechanical strength. Several metastable alumina forms are also known, most of which have a defective spinel-type structure. These phases (called γ, δ-, η, and θ) are characterized by different ordering of the cation vacancies arising from the defect with respect to the ideal spinel stoichiometry MAl_2O_4 (M, bivalent cation). They are much more active than corundum as catalysts mainly due to their Lewis acidic properties, related to the presence only on these phases of tetrahedrally coordinated Al^{3+} cations (*4–6*). Recently, amorphous aluminas have also been the object of surface studies (*7, 8*), and have revealed poor surface reactivity which has been attributed to the octahedral coordination of Al^{3+}.

Metal aluminates are also materials of interest from the surface activity point of view. Several of them are characterized by the spinel structure. In normal spinels Al^{3+} ions are almost completely located in octahedral sites and the surface acidity of these materials is forecast to be weak, at least from the point of view of the abundance of sites. The surface properties of the normal spinels $MgAl_2O_4$ (*9, 10*) and $ZnAl_2O_4$ (*10*) have been investigated previously. Few metal aluminates having the inverse spinel structure exist and their surface chemistry is little known so far; one can forecast that they will act as significantly acidic materials because nearly half of Al^{3+} ions are expected to be in tetrahedral coordination.

To have a more complete picture of the surface chemistry of spinel-type alumina-based materials we have prepared samples of two transition metal aluminates, $NiAl_2O_4$ and $CoAl_2O_4$, having the inverse and the normal spinel structure, respectively (*11–13*). The

---

[1] On leave from Departamento de Química Inorgánica, Universidad de Salamanca, Spain.

0021-9517/91 $3.00

surface properties of these materials are of interest in relation to their possible formation by solid-state reactions in alumina-supported Ni and Co metal catalysts for steam cracking and CO hydrogenation and of Ni–Mo/Al_2O_3 and Co–Mo/Al_2O_3 catalysts for hydrotreating, as well as to their possible use as supports or adsorbents. The surface chemistry of these aluminates, little known in the literature (*14*, *15*), has been studied in comparison with a commercial defective-spinel Al_2O_3 using FT–IR techniques.

EXPERIMENTAL

Materials

Ni and Co aluminates have been prepared by coprecipitation starting from stoichiometric water solutions of Al and Ni (or Co) nitrates (Carlo Erba, Milano, Italy). Precipitation has been carried out at pH 9 using ammonium carbonate. The filtered cakes consisted of a Ni–Al hydroxycarbonate amorphous to XRD, and a crystalline pyroaurite-like Co–Al hydroxycarbonate. The precipitates were washed, dried for 3 h at 390 K, and finally calcined at 1073 K for 3 h in the case of $NiAl_2O_4$ (surface area 128 m^2/g), while at 973 K in the case of $CoAl_2O_4$, in order to avoid excessive area loss (52 m^2/g).

The alumina sample was obtained by calcination at 773 K of a "γ-Al_2O_3" preparation from Strem (220 m^2/g). This material was originally a hydroxide.

Characterization Methods

XRD analysis has been carried out using a Philips diffractometer (CuK_α radiation).

FT–IR spectra have been recorded by a Nicolet MX1 instrument, using conventional Pyrex gas-manipulation evacuation lines and liquid nitrogen-cooled/heatable IR cells (NaCl windows). The samples were activated by evacuation at 773 K before adsorption experiments.

RESULTS

Solid State Characterization

The XRD pattern of $NiAl_2O_4$ is compared in Fig. 1 with those of NiO and of Al_2O_3. The intense peaks correspond to those of the spinel $NiAl_2O_4$ (ASTM table 10-339). The absence of detectable diffraction peaks in the region near $d = 1.395$ Å (2θ–67 for the CuK_α radiation) indicates that spinel-type alumina phases are substantially absent (*1*). On the contrary the most intense diffraction peaks of NiO (Fig. 1b) are very weak shoulders, in agreement with the tendency of Ni–Al mixed oxide preparations to form Ni-deficient spinels (*16*), segregating nickel as NiO. According to Wilson and McConnell (*17*) the XRD pattern of our Al_2O_3 material (Fig. 1c) is assignable to the δ-Al_2O_3 phase, although the differences with the pattern of γ-Al_2O_3 are very subtle.

The XRD pattern of $CoAl_2O_4$ corresponded to a very well-crystallized spinel $CoAl_2O_4$ (ASTM table 10-458).

The FT–IR spectra of the samples in the skeletal region are shown in Fig. 2. They also agree with those reported in the literature (*18*, *19*) for the corresponding compounds. As discussed by Tarte (*18*) and Preudhomme and Tarte (*20*) the highest-frequency IR band of a spinel is associated with vibrational modes mainly involving the highest-valency cation. The position of an absorption band in the region 900–700 cm^{-1} in the spectra of $NiAl_2O_4$ and of δ-Al_2O_3 (in this case it corresponds to a shoulder) is indicative of the presence of tetrahedrally coordinated Al^{3+} ions in these structures. In the normal spinel $CoAl_2O_4$ this band is at lower frequency (668 cm^{-1}), as is typical for octahedrally coordinated Al^{3+} (*18*).

Surface Characterization

(*a*) *Surface hydroxy groups*. The IR spectra in the νOH region of nickel and cobalt aluminate after different evacuation treatments are shown in Figs. 3 and 4. The spectrum of $NiAl_2O_4$ after the strongest evacuation treatment (770 K, Fig. 3a) clearly shows three bands near 3790, 3720, and 3670 cm^{-1}, whose intensity increases in this order. They fall in the region typical for non-hydrogen-bonded hydroxy groups. After evacuation at 710 K (Fig. 3b) a much broader band is also detected whose maximum is centered

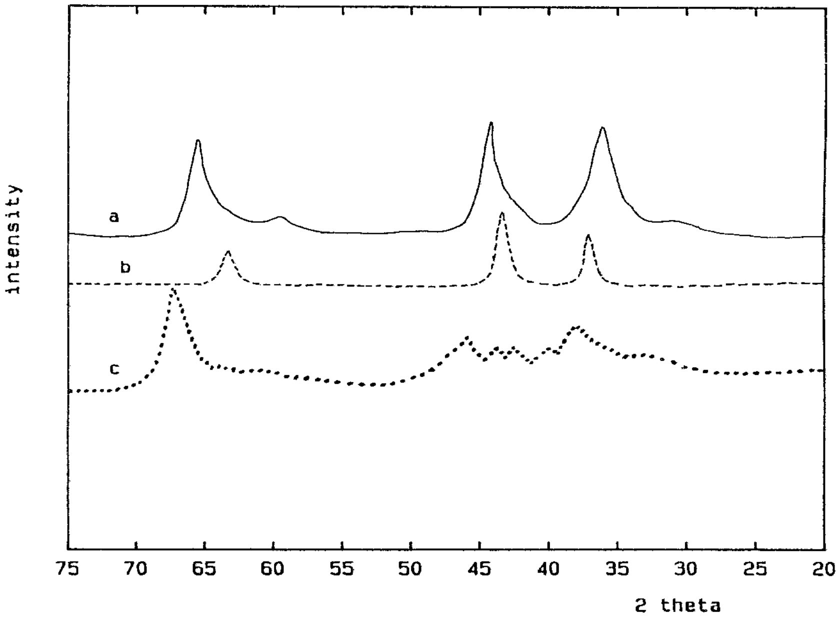

FIG. 1. X-ray diffraction patterns (CuK_α radiation) of (a) $NiAl_2O_4$, (b) NiO, and (c) Al_2O_3.

near 3580 cm^{-1}, due to H-bonded or more perturbed hydroxy groups. There is a remarkable similarity of these spectra with those of δ-Al_2O_3 (Fig. 3c) and of other transition aluminas in similar conditions (*4–6*).

The corresponding spectra of $CoAl_2O_4$ are significantly different (Fig. 4). After evacuation at 773 K there is only one band clearly evident (maximum near 3740 cm^{-1}) with a side component near 3725 cm^{-1}. After weaker evacuation treatments another band is also detected near 3695 cm^{-1}. These spectra have similarities with those of other normal spinels (*9*, *10*) such as magnesium and zinc aluminates. In these cases after strong outgassing a main band (with some shoulders) is observed in the region 3750–3680 cm^{-1}.

(*b*) *Adsorption of pyridine*. Figure 5 compares the spectra obtained after pyridine adsorption (followed by evacuation at increasing temperatures) on the two aluminates as well as on alumina. In the region of the 8a vibrational model (1583 cm^{-1} in the liquid) after evacuation at room temperature (RT) a main band is detected in the case of $NiAl_2O_4$ (Fig. 5A) at 1606 cm^{-1} with a clear compo-

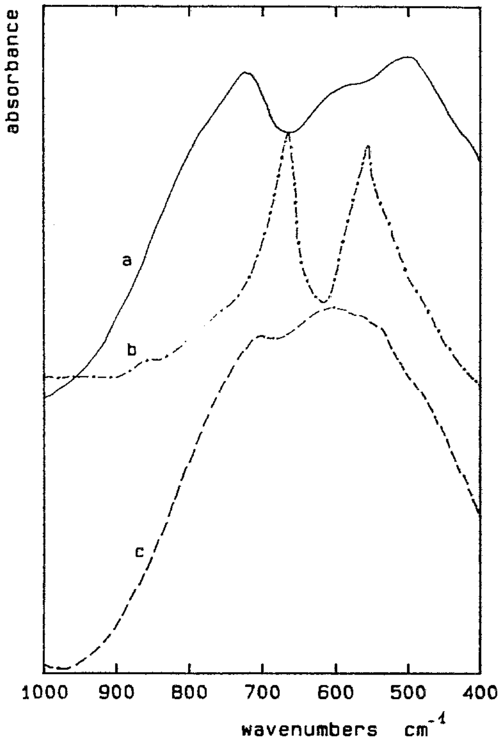

FIG. 2. FT–IR spectra (KBr pressed disks) of (a) $NiAl_2O_4$, (b) $CoAl_2O_4$, and (c) δ-Al_2O_3.

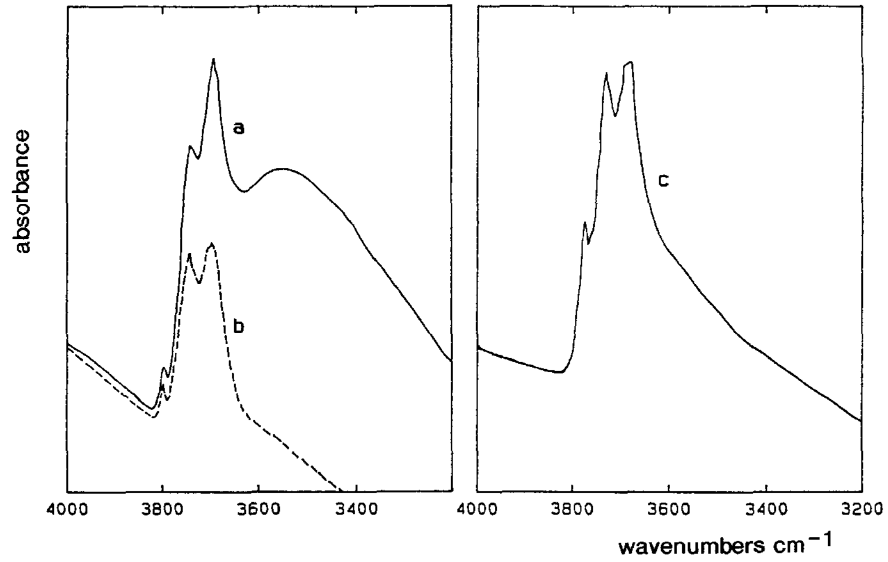

FIG. 3. FT-IR spectra (νOH region) of (a) $NiAl_2O_4$ evacuated at 710 K, (b) $NiAl_2O_4$ evacuated at 770 K, and (c) δ-Al_2O_3 evacuated at 820 K.

nent at 1593 cm^{-1} and a weaker one near 1620 cm^{-1}. The band at 1578 cm^{-1} is due to the 8b component. The effects of evacuation up to 523 K are that the shoulder at 1593 cm^{-1} disappears, due to a weakly bonded species, while the weak band at 1623 cm^{-1} becomes more evident. The main maximum is always detected near 1606 cm^{-1}.

The spectrum of pyridine adsorbed on $CoAl_2O_4$ (Fig. 5B) is similar to that of the nickel compound. In this case the main band is detected near 1608 cm^{-1} and shows a shoulder near 1623 cm^{-1}. A third species, much more labile, is responsible for a ν8a mode at 1595 cm^{-1}, which after evacuation at RT appears much more intense than in the case of the nickel compound. Evacuation at temperatures higher than 423 K causes the transformation of pyridine to a species whose spectrum corresponds to that of 2,2'-bipyridyl (*21*). This reaction is probably related to the oxidizing properties of the cobalt compound, as also shown below.

Also in the spectrum of pyridine adsorbed on δ-Al_2O_3 under the same conditions (Fig. 5C) we can identify three bands belonging to the 8a vibration. The band near 1595 cm^{-1} disappears by evacuation at 423 K; the main band, even at 523 K, is at 1617 cm^{-1} with an unresolved component near 1622 cm^{-1}. The behavior is similar to that reported by Morterra *et al.* for η-Al_2O_3 (*22*).

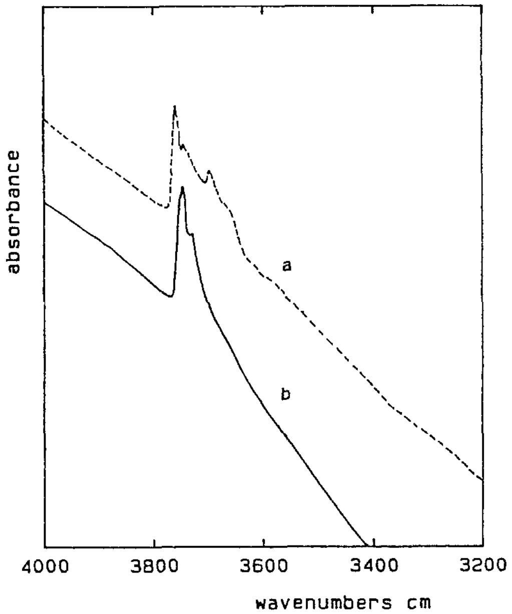

FIG. 4. FT-IR spectra (νOH region) of $CoAl_2O_4$ evacuated at (a) 710 (K) and (b) 770 K.

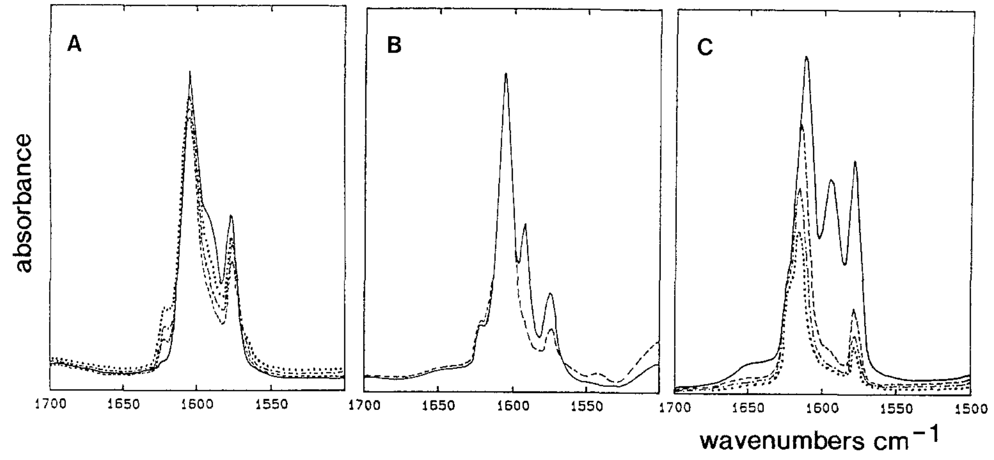

FIG. 5. FT–IR spectra of pyridine (8a and 8b vibrational modes) adsorbed on (A) $NiAl_2O_4$, (B) $CoAl_2O_4$, and (c) δ-Al_2O_3 followed by evacuation at RT (solid lines), at 423 K (broken lines), at 473 K (point lines), and 523 K (dashed lines).

(*c*) *Adsorption of carbon monoxide*. The IR spectra of CO adsorbed on $NiAl_2O_4$ at RT at different coverages are shown in Fig. 6. Two bands are observed, having different behavior. The higher frequency band has its maximum at 2185 cm^{-1} at the highest coverages, decreasing rapidly in intensity as coverage is reduced and shifting to near 2195 cm^{-1} at the lowest coverages. By decreasing the coverage a distinct shoulder also appears, near 2207 cm^{-1}. The spectrum at low coverages resembles that detected on δ-Al_2O_3 (insert in Fig. 6), as on several transitional aluminas (*23–25*), although shifted downward by nearly 15 cm^{-1}. On aluminas, in fact, two weak bands are observed near 2235 and 2210 cm^{-1}. Bands in these positions are certainly associated with CO bonded to Al^{3+}-exposed ions of high Lewis acidity.

Another band, more resistant to evacuation, is observed on $NiAl_2O_4$, at lower frequencies. However, as will be shown elsewhere (*26*), this band is not detected by contact at lower temperatures. This band, showing two components at 2130 and 2100 cm^{-1}, falls at lower frequencies with respect to gas-phase CO and consequently involves carbonyls on cations having *d*-type elec-

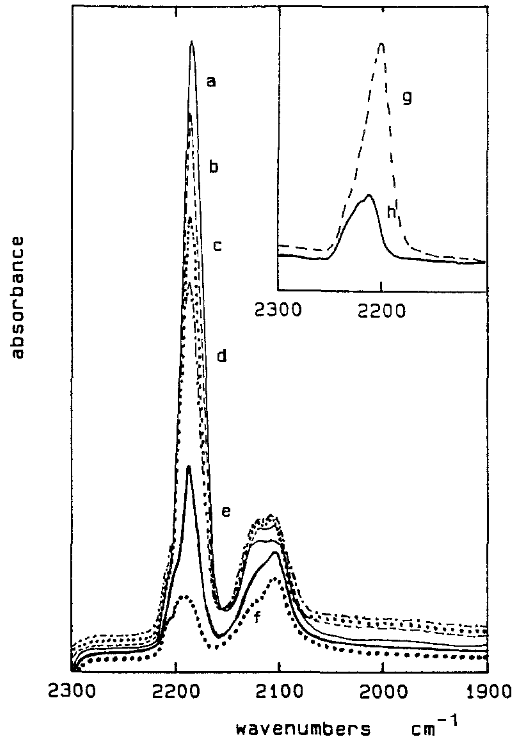

FIG. 6. FT–IR spectra of CO adsorbed on $NiAl_2O_4$ at RT in contact with CO gas at (a) 65 Torr, (b) 30 Torr, (c) 10 Torr, (d) 1 Torr, (e) 0.1 Torr, and (f) after short evacuation. In the insert, FT–IR spectra of CO adsorbed on δ-Al_2O_3 under evacuation at 273 K (g) and 293 K (h).

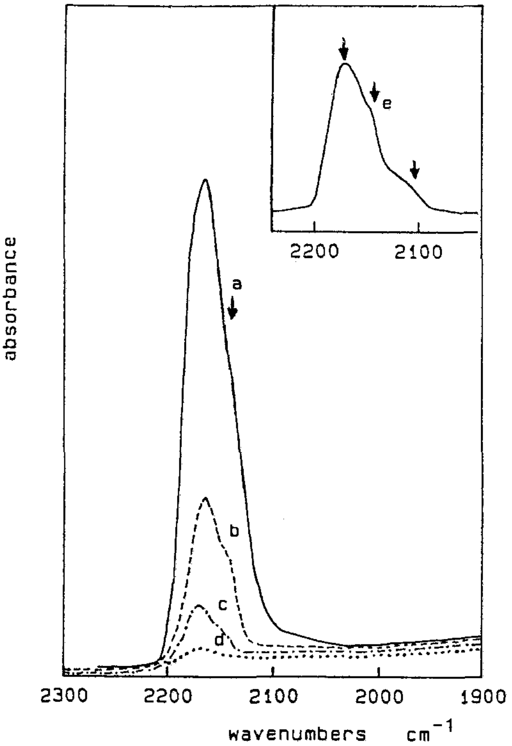

FIG. 7. FT–IR spectra of CO adsorbed on $CoAl_2O_4$ after contact with CO gas at 170K and evacuation at (a) 170 K, (b) 250 K, (c) 273 K, and (d) 290 K. In the insert: FT–IR spectrum of CO after brief contact with $CoAl_2O_4$ at RT.

trons, such as Ni^{2+} or more reduced Ni centers. From the behavior of this band we assign it to CO interacting with Ni^{+} centers, produced by reduction of Ni^{2+} by CO (*27*). Low temperature adsorption experiments provide evidence that the main band near 2185 cm^{-1} shows a shoulder near 2160 cm^{-1}, probably due to carbonyl species on Ni^{2+} sites (*26*).

CO adsorbed on $CoAl_2O_4$ at RT (insert in Fig. 7) is responsible for a main band with maximum at 2170 cm^{-1} and a shoulder near 2140 cm^{-1}, with also a weaker component near 2100 cm^{-1}. On increasing the time of contact the spectrum is readily modified with the growth of bands in the region 2120–1950 cm^{-1} and also of absorption in the carbonate region. As already observed in the case of other cobalt compounds such as Co_3O_4 (*28*) and $CoCr_2O_4$ (*29*) these modifications are associated with redox reactions. Adsorbed CO is oxidized to CO_2 and carbonates, while other CO molecules adsorb giving carbonyls or polycarbonyls on reduced cobalt centers Co^{+} or Co^{0}. In order to inhibit this redox process, we have carried out the CO adsorption experiment also at lower temperatures (Fig. 7a–d). In these conditions only the main band is observed, again composed of two absorptions centered near 2170 cm^{-1} and 2140 cm^{-1}. The two components have similar stabilities and decrease together by evacuation upon warming, without important shifts. An extremely weak component can also be seen near 2210 cm^{-1}. According to previous studies, the band at 2140 cm^{-1} is probably due to CO on Co^{2+} centers (*28, 29*), while that near 2170 cm^{-1} is probably due to be assigned to CO on octahedrally coordinated Al^{3+} exposed ions (*25*). The extremely weak band near 2210 cm^{-1} is possibly due to CO on tetrahedral Al^{3+}, as discussed above in relation to pyridine adsorption.

(*d*) *Surface metal–oxygen vibrations*. In the case of transitional aluminas it has been previously shown (*30–32*) that surface metal–oxygen modes are responsible for a broad absorption in the region 1150–1000 cm^{-1}, centered near 1060 cm^{-1}, immediately above the cut-off limit of pure powder pressed disks, due to the bulk metal–oxygen absorptions. These modes are relaxed by adsorption of basic molecules, such as pyridine, resulting in the disappearance of these absorptions due to being shifted down and no longer detectable. For this reason we have investigated the effect of pyridine adsorption on the low-frequency spectral region. The cut-off limit is only slightly lower on $NiAl_2O_4$ (960 cm^{-1}) than on Al_2O_3 (near 1000 cm^{-1}), because on both materials tetrahedral Al cations are present, responsible, as discussed above, for bulk absorptions at frequencies higher than those of octahedral Al cations. Accordingly, on $CoAl_2O_4$ the cut-off limit is distinctly lower (880 cm^{-1}). On both aluminates surface modes are ob-

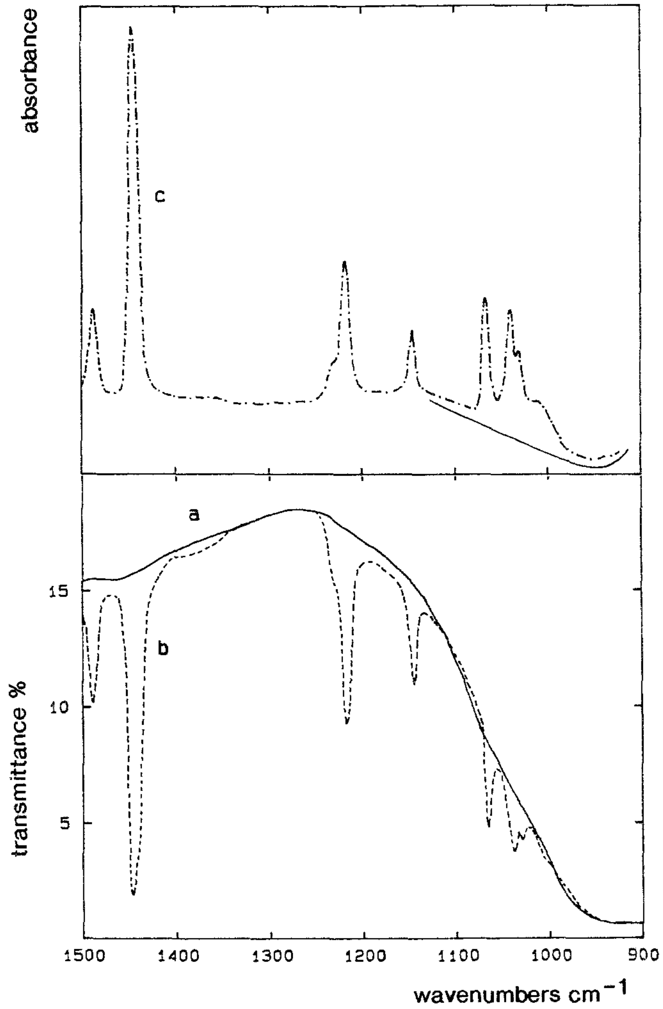

FIG. 8. Transmittance IR spectra of $NiAl_2O_4$. (a) activated at 773 K, and (b) after contact with pyridine (2 Torr) at RT and successive evacuation at RT. Spectrum (c) is the subtraction (b) –(a), expressed in absorbance. Full line in the upper spectrum: evidence for a broad negative band in the region 1100–900 cm^{-1} (see text).

servable, responsible for broad absorptions that disappear (and can be seen as negative absorptions in the difference spectra) upon pyridine adsorption. In both cases these bands extend from near 1200 cm^{-1} to the cut-off. This is shown in Fig. 8 in the case of $NiAl_2O_4$.

DISCUSSION

The most significant spectral features arising from surface hydroxy groups and adsorbed carbon monoxide and pyridine on the three aluminate compounds under study are summarized in Table 1. The assignments proposed are also reported, based on the discussion given below.

$NiAl_2O_4$, $CoAl_2O_4$ and δ-Al_2O_3 have in common the basic spinel-type structure, being, respectively, an inverse, a normal, and a defective spinel. The structure of δ-Al_2O_3 is a defective form of the spinel structure and can be described by the structural nota-

TABLE 1

Assignments of IR Bands of Surface Species

Surface species	Vibrational mode	Wavenumbers (cm^{-1})	Structure[a]
Hydroxy-groups	νOH Type Ib[a]	~3790	$_4Al^{3+}$–OH
	Type Ia[b]	~3770	□–O–$_4Al^{3+}$–OH
	Type II[b]	~3730	$_6Al^{3+}$–OH
		3750–3680	M^{2+}–OH
	Type III[b]	~3680	Bridging
		~3580	Triply bridging
Coord. pyridine	8a Type I[c]	~1625	$_4Al^{3+} \leftarrow$ py
	Type II[c]	~1615	□—O–$_4Al^{3+} \leftarrow$ py
		1608–1605	$_4M^{2+} \leftarrow$ py
	Type III[c]	~1595	$_6M^{n+} \leftarrow$ py
Coord. CO	νCO	2240–2210	$_4Al^{3+} \leftarrow$ CO
		2200–2180	$_6Al^{3+} \leftarrow$ CO
		2170–2140	$M^{2+} \leftarrow$ CO

Note. □, Cation vacancies.

[a] Subscripts: coordination numbers.

[b] Notations from Knözinger and Ratnasamy (*4*).

[c] Notations from Morterra *et al.* (*22*).

tion $(Al_8)[Al_{13\frac{1}{3}}\square_{2\frac{2}{3}}]O_{32}$, where octahedrally and terahedrally coordinated sites are enclosed in square and round brackets, respectively, and the square symbol denotes cationic vacancies with respect to the ideal spinel structure. According to Wilson and McConnell (*17*), in δ-Al_2O_3 cation vacancies are essentially located in octahedral sites. Using the same notations, and according to the disorder found in both $CoAl_2O_4$ (nearly 80% normal (*11*)) and $NiAl_2O_4$ (nearly 80% inverse (*12, 13*)), these spinels can be denoted as $(Co_{6.4}Al_{1.6})[Al_{14.4}Co_{1.6}]O_{32}$ and $(Al_{6.4}Ni_{1.6})[Al_{9.6}Ni_{6.4}]O_{32}$, respectively.

The spectra of $NiAl_2O_4$ and δ-Al_2O_3 in the νOH region are very similar, showing three bands in the 3800–3650 cm^{-1} region. This suggests that the surface structures responsible for the bands are the same. The spectrum of $CoAl_2O_4$ in the νOH region, instead, is similar to that of the other normal spinels $MgAl_2O_4$ (*9, 10*) and $ZnAl_2O_4$ (*10*). After strong evacuation, bands are only present in the region 3750–3690 cm^{-1} (in this case the main band is at 3740 cm^{-1} with a weaker one at 3725 cm^{-1}). A band near 3695 cm^{-1} is also detected and much more labile than in the other cases.

Knözinger and Ratnasamy (*4*) identified five bands due to surface free OHs of transitional aluminas. They assigned bands in the region 3760–3800 cm^{-1} to OHs coordinated to a single Al^{3+} ion, either octahedral (3785–3800 cm^{-1}, type Ib) or tetrahedral (3760–3780 cm^{-1}, type Ia). They also found a double band between 3735 and 3745 cm^{-1} and assigned the components to OHs bridging between two Al^{3+} ions either both octahedral (3740–3745 cm^{-1}, type IIb) or one tetrahedral and one octahedral (3730–3735 cm^{-1}, type IIa). A fifth band placed near 3700 cm^{-1} has been assigned to triply bridging OHs (type III).

Hence, type II bands (3750–3720 cm^{-1}) are present in the spectra of normal, inverse, and defective aluminate spinels. Instead type I and III bands, detected on aluminas and $NiAl_2O_4$, are not detected on normal spinels. It seems very reasonable to associate both type I and III bands to tetrahedral Al^{3+} cations. Consequently, with a modification of the Knözinger–Ratnasamy model (*4*) we assign for $NiAl_2O_4$ and δ-Al_2O_3 band I (3790 cm^{-1}) to OHs coordinated on a single tetrahedral Al^{3+} cation, band II (3740 cm^{-1}) to OH's coordinated on a single octahedral Al^{3+} cation, and band III (3680 cm^{-1}) to OHs bridging over a couple of cations, one of which has tetrahedral coordination. OHs bonded to Ni^{2+}, probably more labile than the AlOH ones, are expected to fall in the region 3740–3680 cm^{-1}, as on NiO (*26, 33*): they can be absent or could contribute to type II and III bands. The bands at 3750 and 3725 cm^{-1} detected in the spectrum of $CoAl_2O_4$ can be associated to OHs bonded to octahedral Al^{3+} and tetrahedral Co^{2+}, respectively. In this case, with tetrahedral Al^{3+} ions *almost absent,* bridging OHs probably responsible for the band near 3680 cm^{-1} should be more weakly bonded and would be labile and disappear by evacuation at 773 K.

Our assignments are supported by the comparison with the spectra of metal–hydroxo complexes having different coordination of the OH group. Literature data show that non-H-bonded bridged OHs, such as those of the complexes $[(CH_3)_2Ga(OH)]_3$ (*34*) and $[(CH_3)_3Sn(OH)]_\infty$ (*35*), are characterized by νOH bands near 3640 cm^{-1}, while triply briding OHs, as in the case of the complex $[(CH_3)_3Pt(OH)]_4$ (*36*), show bands at even lower frequencies (3595 cm^{-1}). On surfaces, triply bridging OHs are expected to absorb below 3600 cm^{-1}, as is thought for other oxides such as ThO_2 (*37*). On the other hand, νOH frequencies are also sensitive to the nature of the bonded cations (weight and electronic structure), as is well known for terminal hydroxides (*38*) and also appears evident, for example, if the spectra of the three isostructural brucite-type hydroxides $Mg(OH)_2$, $Ca(OH)_2$ (*39*), and $Co(OH)_2$ (*40*) are compared. In these cases all hydroxy groups are triply bridging and non-H-bonded but vibrationally coupled. So they are responsible for a strong IR active band at 3700, 3644, and 3630 cm^{-1} for Mg, Ca, and Co compounds, respectively, while a second band is Raman active at lower frequencies (3655 cm^{-1} for the Mg compound and 3618 cm^{-1} for the Ca compound). Summarizing, these data should indicate that the OH frequency of surface hydroxy groups depends inversely on the coordination (linear > bridging > triply bridging), according to Knözinger and Ratnasamy (*4*), and from the electronegativity and from the weight of the bonded cations. As for Al^{3+} compounds, we can refer to the spectra of some Al^{3+}-containing layered silicates, which contain non-H-bonded hydroxy groups bridging over two Al^{3+} ions, such as pyrophyllite and kaolinite. These materials can show more than one band due to coupling in the region 3720–3620 cm^{-1} (*41*). In particular pyrophyllite ($Al_2Si_4O_{10}(OH)_2$) shows a sharp intense band at 3675 cm^{-1}, with a weak shoulder near 3650 cm^{-1} (*41*). According to these data it seems reasonable to assign a broadband near 3580 cm^{-1}, detected on incompletely dried aluminas as well as on Ni Al_2O_4, to triply bridging OHs, while OHs bridging over two cations can be responsible for type III bands (3700–3640 cm^{-1}).

The splitting of the type I band (and perhaps also of band II) in δ-Al_2O_3 and on most transitional aluminas is likely to be relative to the presence of cation vacancies only on these materials. The OH bonded to a single Al^{3+} ion could be sensitive to the presence of cationic vacancies in the nearest sites, because in this case the basicity of the oxide ligands constituting the coordination sphere of a cation in tetrahedral coordination can be much enhanced. To support this idea we mention that, following Tsyganenko *et al.* (*42*), the cation vacancies in incompletely dehydroxylated spinel aluminas can be occupied by H^+ ions, producing internal OHs. Both Zecchina *et al.* (*6*) and Lavalley *et al.* (*24*) showed that the splitting of type I bands with the appearance of the band at 3770 cm^{-1} (Ia following Knözinger and Ratnasamy (4)) is associated with some kind of "hydrothermal" treatment, being absent in samples not treated in wet environments.

The spectrum of pyridine on transition aluminas has been discussed by Morterra *et al.* (*22*). They observed three adsorbed species characterized by three bands due to the 8a vibration mode (1583 cm^{-1} in liquid pyridine). These authors assigned type I (1623 cm^{-1}) and type III (1595 cm^{-1}) bands to pyridine species coordinated on a tetrahedral and an octahedral Al^{3+} cation, respectively, both coordinatively unsaturated. Type II bands (1617 cm^{-1}) have been assigned tentatively to pyridine bridging over two cations, one octahedral and one tetrahedral.

On $NiAl_2O_4$ type I and III bands are also observed, and can be assigned in the same way. A third band is also observed, but its frequency (1605 cm^{-1}) suggests its assignment to pyridine bonded to Ni^{2+}. Type II band of aluminas (1615 cm^{-1}) is not observed on stoichiometric spinels. This suggests that the type II band is associated with a structure present only on defective spinel-type structures, like aluminas. According to the apparent tendency to cation vacancy clustering in the series $\gamma \rightarrow \delta \rightarrow \theta$ Al_2O_3 (*17, 43*), this band can be associated with pyridine coordinated on a single tetrahedral

Al^{3+} cation placed near cation vacancy clusters. This situation would justify the Lewis acidic nature of these sites, weaker than those characterizing type I sites because some of their oxide ligands should be more basic, as proposed above.

According to the above assignments the bands of pyridine adsorbed on $CoAl_2O_4$ should correspond to species bonded to octahedral Al^{3+} (1595 cm^{-1}, type III) and to Co^{2+} (1608 cm^{-1}), while the band at 1623 cm^{-1} should correspond to pyridine on tetrahedral Al^{3+}, present because of the partial inversion of this spinel structure. The relative intensity of the bands detected on cobalt and nickel aluminates after evacuation at RT provides evidence that on the cobalt compound the ratio between type I and type III bands (indicative of the tetrahedral/octahedral Al^{3+} ratio at the surface) is indeed much smaller than on the nickel compound, as expected. However, because of the different extinction coefficients of the bands in different surface species, we cannot assess whether the ratio at the surfaces reflects that in the bulk or is different, as proposed previously (*14*).

The spectra of CO adsorbed on the three compounds are in good agreement with the indications arising from pyridine adsorption. The weak band in the region 2210–2190 cm^{-1} present on the inverse spinel corresponds to those found at 2230–2210 cm^{-1} on aluminas and is very likely to be indicative of CO interacting with tetrahedral Al^{3+} sites. This band is extremely weak on the normal spinel, according to the small amount of the tetrahedral Al and the intrinsic weakness of the band. On $CoAl_2O_4$ a main band in the region 2175–2165 cm^{-1} reveals instead octahedral Al^{3+} sites to be predominant.

As discussed above, these bands can be distinguished from those associated with CO interacting with Ni^{2+} and Co^{2+} cations. Moreover, it is evident that at RT CO reduces both Co^{2+} and Ni^{2+} ions at the surface. Thus CO adsorption experiments show that Ni and Co ions are indeed exposed on the surface of their aluminates, as expected, in contradiction with data arising from the ISS technique (*14*).

CONCLUSIONS

The comparative IR study of the surface properties of cobalt aluminate (an essentially normal spinel), nickel aluminate (an essentially inverse spinel) and δ-Al_2O_3 (a defective spinel) has allowed us to establish that the surface structures of these materials reflect qualitatively those of the bulk, so exposing the cations in the same coordination state as in the bulk, although incomplete.

The results of our investigation suggested also slight modifications of the criteria previously used for the assignments of the bands of surface OHs of aluminas, discussed thoroughly by Knözinger and Ratnasamy (*4*) and of adsorbed pyridine on alumina, mainly due to Morterra *et al.* (*22*). The discussion reported above is based on assumptions similar to those of Knözinger and Ratnasamy (*4*). However, the comparison of the available data is in favor of the assignments given in Table 1. From this interpretation, bridging and triply bridging OHs on aluminas are thought to be responsible for bands (near 3670 and 3580 cm^{-1}) at frequencies lower than previously thought, the latter ones being so labile as to be destroyed by evacuation at temperatures higher than 773 K. The comparison of the spectra recorded on stoichiometric spinels and defective spinel aluminas also suggests that in the latter some OHs and Lewis sites are present which are lacking in the former. In fact only on aluminas "type I" are νOH bands split and "type II" adsorbed pyridine is detected. We propose that the sites responsible for these features are placed near cation vacancy clusters in the defective spinel-type Al_2O_3 structure, their activity being modified with respect to the structural sites of spinels because of the higher basicity of oxide ions surrounding the Al^{3+} ions adjacent to cation vacancies.

ACKNOWLEDGMENTS

This work has been supported by MURST (Italian Ministry for University and Scientific and Technological Research "40% funds"). One of the authors (V.S.E.) acknowledges the Spanish Government for a research grant.

REFERENCES

1. Lippens, B. C., and Staggerda, J. J., *in* "Physical and Chemical Aspects of Adsorbents and Catalysts" (B. G. Linsen, Ed.), p. 171. Academic Press, New York, 1970.
2. Poisson, R., Brunelle J. P., and Nortier, P., *in* "Catalyst Supports and Supported Catalysts" (A. B. Stiles, Ed.), p. 11. Butterworths, Boston, 1987.
3. Oberlander, R. K., *in* "Applied Industrial Catalysis" (B. E. Leach, Ed.), p. 64. Academic Press, New York, 1984.
4. Knözinger, H., and Ratnasamy, P., *Catal. Rev.* **17,** 31 (1978).
5. Zecchina, A., Garrone, E., and Guglielminotti, E., *in* "Catalysis," Vol. 6, p. 90. Royal Society of Chemistry, London 1983.
6. Zecchina, A., Coluccia, S., and Morterra, C., *Appl. Spectrosc. Rev.* **21,** 259 (1985).
7. Abbattista, F., Del Mastro, S., Gozzellino, G., Mazza, D., Vallino, M., Busca, G., Lorenzelli, V., and Ramis, G., *J. Catal.* **117,** 42 (1989).
8. Nortier, P., Fourre, P., Mohammed Saad, A. B., Saur, O., and Lavalley, J. C., *Appl. Catal.* **61,** 141 (1990).
9. Morterra, C., Ghiotti, C., Boccuzzi, F., and Coluccia, A., *J. Catal.* **51,** 299 (1978).
10. Rossi, P. F., Busca, G., Lorenzelli, V., Saur, O., and Lavalley, J. C., Langmuir, in press.
11. Angeletti, C., Pepe, F., and Porta, P., *J. Chem. Soc. Faraday Trans. 1,* **72,** 1971 (1977).
12. Porta, P., Stone, F. S., and Turner, R. G., *J. Solid State Chem.* **11,** 135 (1974).
13. Mocala, K., and Navrotsky, A., *J. Am. Ceram. Soc.* **72,** 826 (1989).
14. Shelef, M., Wheeler, M. A. Z., and Yao, H. C., *Surf. Sci.* **47,** 697 (1975).
15. Gil-Llambias, F. L., Escueley Castro, A. M., and Santos Blanco, J., *J. Catal.* **83,** 225 (1983).
16. Bassoue, P., Lefebvre, A., and Gelles, J. C., *J. Solid State Chem.* **10,** 56 (1974).
17. Wilson, S. J., and McConnell, J. D. C., *J. Solid State Chem.* **34,** 315 (1980).
18. Tarte, P., *Spectrochim. Acta Part A* **23,** 2127 (1967).
19. Baraton, M. I., and Quintard, P., *J. Mol. Struct.* **79,** 337 (1982).
20. Preudhomme, J., and Tarte, P., *Spectrochim. Acta Part A* **28,** 69 (1972).
21. Busca, G., and Lorenzelli, V., *Mater. Chem.* **6,** 175 (1981).
22. Morterra, C., Chiorino, A., Ghiotti, G., and Garrone, E., *J. Chem. Soc. Faraday Trans. 1,* **75,** 271 (1979).
23. Della Gatta, G., Fubini, B., Ghiotti, G., and Morterra, C., *J. Catal.* **43,** 90 (1976).
24. Lavalley, J. C., Benaissa, M., Busca, G., and Lorenzelli, V., *Appl. Catal.* **24,** 249 (1986).
25. Zecchina, A., Escalona Platero, E., and Otero Areán, C., *J. Catal.* **107,** 244 (1987).
26. Busca, G., Lorenzelli, V., Guidetti, R., and Sanchez Escribano, V., submitted for publication.
27. Kermarek, M., Olivier, D., Richard, M., Che, M., and Bozon-Verduraz, F., *J. Phys. Chem.* **86,** 2818 (1982).
28. Busca, G., Guidetti, R., and Lorenzelli, V., *J. Chem. Soc. Faraday Trans. 1,* **86,** 989 (1990).
29. Busca, G., Trifirò, F., and Vaccari, A., *Langmuir* **6,** 1440 (1990).
30. Morterra, C., *in* "Proceedings, 6th International Congress on Catalysis, London, 1976" (G. C. Bond, P. B. Wells, and F. C. Tompkins, Eds.), p. 193. Chemical Society, London, 1977.
31. Lavalley, J. C., and Benaissa, M., *J. Chem. Soc. Chem. Commun.,* 908 (1984).
32. Zecchina, A., and Scarano, D., *in* "Adsorption and Catalysis on Oxide Surfaces" (M. Che, and G. C. Bond, Eds.), p. 71. Elsevier, Amsterdam, 1985.
33. Tsyganenko, A. A., and Filimonov, V. N., *J. Mol. Struct.* **19,** 579 (1973).
34. Thomas, R. J., *Inorg. Chem.* **7,** 1714 (1968).
35. Brown, J. M., *J. Chem. Soc. Dalton,* 338 (1972).
36. Bulliner, P. A., and Spiro, T. G., *Inorg. Chem.* **8,** 1023 (1969).
37. Montagne, X., Lynch, J., Freund, E., Lamotte, J., and Lavalley, J. C., *J. Chem. Soc. Faraday Trans. 1,* **83,** 1417 (1987).
38. West, R., and Baney, R. H., *J. Phys. Chem.* **64,** 822 (1960).
39. Freund, F., *Spectrochim. Acta Part A* **26,** 195 (1970).
40. Vincent, F., Figlarz, M., and Amiel, J., *in* "Reactivity of Solids" (J. W. Mitchell, *et al.,* Eds.), p. 181. Wiley, New York, 1968.
41. Farmer, V. C., and Russel, J. D., *Spectrochim. Acta* **20,** 1149 (1964).
42. Tsyganenko, A. A., Smirnov, K. S., Rzhevskii, A. M., and Mardilovich, P. P., *Mater. Chem. Phys.* **26,** 35 (1990).
43. Wilson, S. J., *Proc. Br. Ceram. Soc.* **28,** 281 (1979).